PosterGate

Cite: PosterGate, 2019, L0K18002, www.PosterGate.net

Integrating 3D Bioprinting and Biologically Inspired Nanomaterials for Complex Tissue Regeneration

Lijie Grace Zhang

Department of Mechanical and Aerospace Engineering and Department of Medicine,

The George Washington University, Washington, DC 20052.

INTRODUCTION

Cells within the human body are in intimate contact with a 3D nanostructured extracellular matrix composed of numerous organic and inorganic components. As a result, one of the revolutionary changes in the field of biomaterials and tissue engineering is to develop biologically inspired nanomaterials and advanced 3D biofabrication techniques to create complex tissue construct mimicking native tissue. However, related studies are limited. As an emerging technique for custom fabricated tissue constructs, 3D bioprinting holds great potential to create highly functional tissues and organs with spatiotemporally organized bioactive cues, desirable patient-specific geometry, and well-controlled architecture. Therefore, the main objective of our research is to develop novel biologically inspired nanomaterials and advanced 3D bioprinting techniques to fabricate the next generation of nano tissue scaffolds for complex tissue regeneration

Design of Novel Nanomaterials

Nanomaterials (I): Hydrothermally Treated Nanocrystalline Hydroxyapatites (nHA)

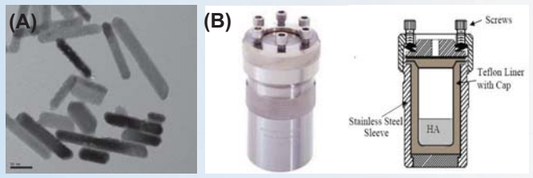

Nanomaterials (II): A DNA-based Self-Assembly Rosette Nanotubes (RNTs)

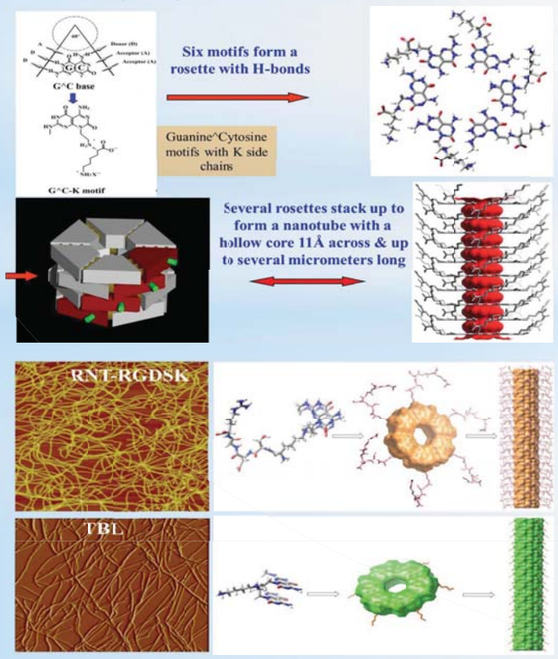

RNTs for Cartilage and Bone Regeneration

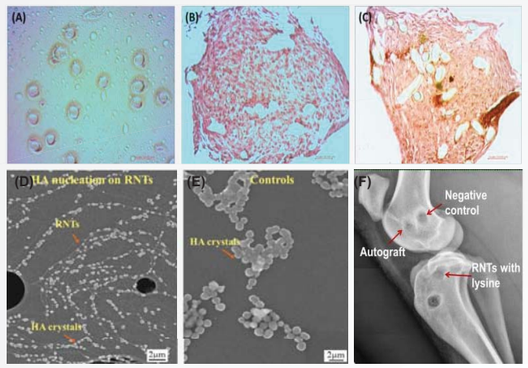

Figure 1. H&E staining of (A) controls; (B) RNTs with aminobutane linker and (C) RNTs with RGDSK for improved cartilage regeneration. (D) Scanning electron microscopy (SEM) image of nHA nucleation on RNTs into a bone like pattern and (E) nHA only. (F) X-ray image of improved bone regeneration on RNT hydrogel (39.8 of X-ray intensity) when compared to autograft (28.8), and negative blank controls (17.8) after 8 week implantation into the femur and tibia of pigs.

3D Bioprinting

Figure 2. Schematic illustration of several 3D printers.

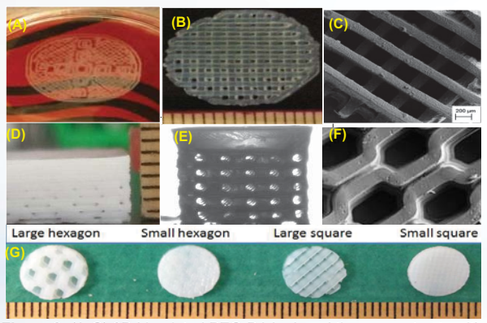

Figure 3. (A-G) 3D bioprinted PEG-DA hydrogel tissue constructs with varied designs fabricated in our lab. SEM images of 3D bioprinted constructs (C) with nHAs and (F) with hexagonal pores.

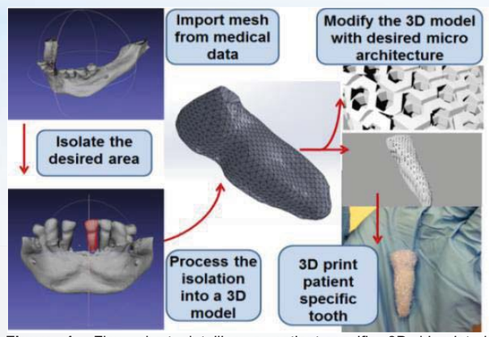

Figure 4.. Flow chart detailing a patient-specific 3D bioprinted construct design process, with a frontal incisor as an example.

3D Printed Osteochondral Construct

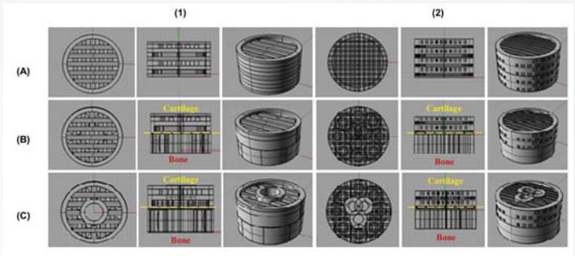

Figure 5. CAD images of the (1) large and (2) small pore model and (A) homogeneous, (B) bi-phasic and (C) bi-phasic key featured osteochondral construct designs.

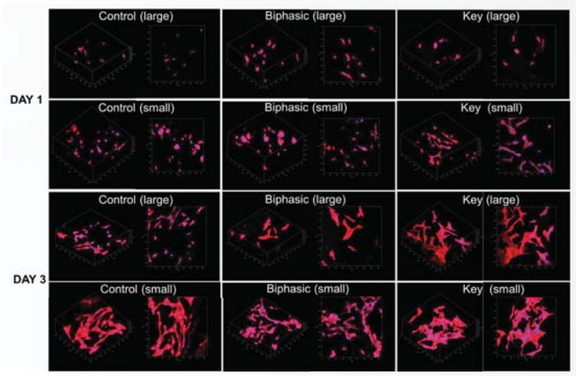

Figure 6. Confocal microscopy images of human bone marrow mesenchymal stem cell (hMSC) growing on 3D printed scaffolds after 1 and 3 days of culture.

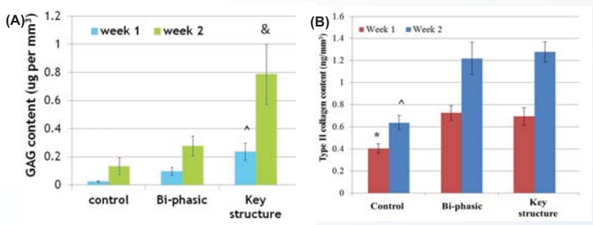

Figure 7. (A) Glycosaminoglycan (GAG) synthesis in various 3D printed osteochondral scaffolds. Data are ± standard error of the mean, n=9; &p<0.05 when compared to all other scaffolds and ^p<0.05 when compared to controls and bi-phasic scaffolds after 1 week. (B) Collagen type II synthesis. *p<0.05 and ^p<0.05 when compared to all other scaffolds at respective weeks.

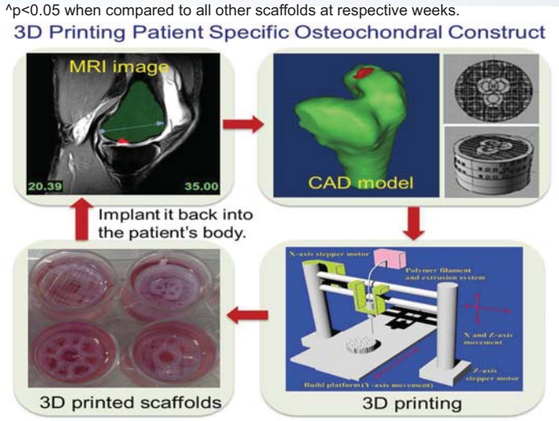

Figure 8. 3D printing patient-specific scaffolds with designed internal structures for osteochondral defect treatment.

3D Printed Vascularized Bone

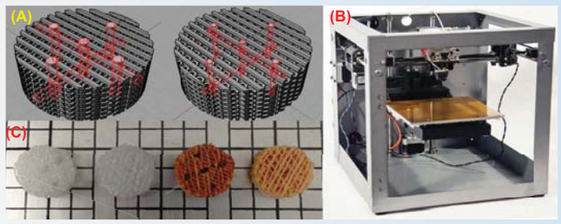

Figure 9. (A) 3D CAD designs (B) our printer (C) 3D printed and nHA modified scaffolds.

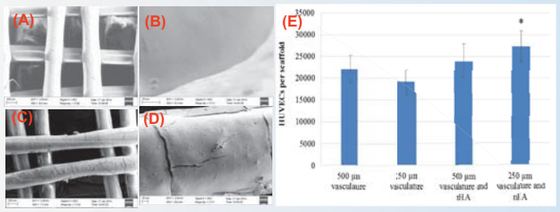

Figure 10. SEM images of printed scaffolds (A-B) without nHA and (C-D) with nHA at low and high magnification. (C) Human umbilical vein endothelial cell adhesion; n=9; *p<0.05 when compared to scaffolds with 250 μm vasculature.

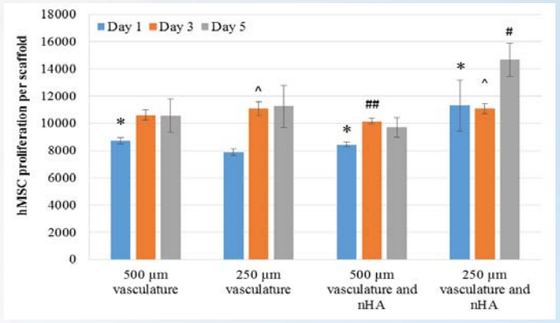

Figure 11; Improved hMSC proliferation on 3D printed scaffolds with nHA and small vasculature; #p<0.01 when compared to all other scaffolds at day 5 and ##p<0.05 when compared to 500 and 250 μm vasculature without nHA; ^p<0.05 when compared to scaffolds with 500 μm vasculature and nHA at day 3; and *p<0.05 when compared to scaffolds with 250 μm vasculature at day 1.

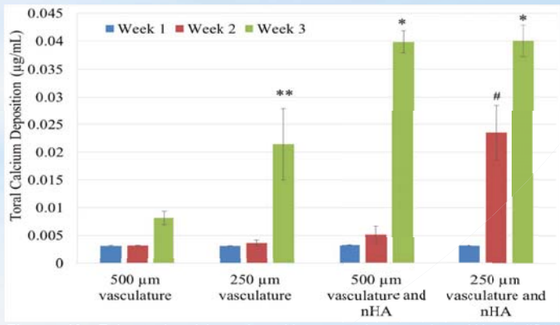

Figure 12. Enhanced calcium deposition on microvascular nHA modified scaffolds after 3 weeks. *p<0.05 when compared to 3D printed bone scaffolds with 500 and 250 μm vasculature at week 3; **p<0.05 when compared to 3D printed bone scaffolds with 500 μm vasculature at week 3; #p<0.01 when compared to all other scaffolds at week 2.

ACKNOWLEGEMENT

The authors would like to thank NIH Director's New Innovator Award for financial support.